TECHNICAL RESEARCH REPORT

The Mechanics of Material Removal Mechanisms in the Machining of Ceramics

by G.M. Zhang, K.G. Satish, and W.F. Ko

T.R. 94-22r1

Sponsored by
the National Science Foundation
Engineering Research Center Program,
the University of Maryland,
Harvard University,
and Industry

The Mechanics of Material Removal Mechanisms in the Machining of Ceramics

Guang M. Zhang, K. G. Satish, and **Wing F. Ko**
Department of Mechanical Engineering and
Institute for Systems Research
University of Maryland
College Park, Maryland

ABSTRACT

This paper presents a study on the mechanics of material removal for ceramic materials by observing single-point turning process of aluminum oxide (Al_2O_3). On-line cutting force measurement is performed and the surface integrity is characterized off-line by examining the surface texture. A theoretical analysis of fracture mechanics provides a comprehensive understanding of the chip formation process, and a model describing the material removal mechanisms is discussed. Based on the model, a systematic investigation of the chip fragments formed during machining is performed.

INTRODUCTION

The growing need for higher strength materials is driving modern industries toward the development of advanced ceramic materials. Ceramic materials' superior resistance to heat , to corrosion, and to wear and abrasion makes them advantageous over other engineering materials. Its capability to be manufactured to near net shape by pressing and sintering processes makes economic production of ceramics possible, yet, machining processes are still needed to ensure dimensional and geometrical accuracy. Unfortunately, ceramic materials are difficult to machine and often fractured during the machining process. Many attempts have been made to assure the quality of the machined ceramic components.

The current research of Chryssolouris et al [1,2] has developed a "laser lathe", that applies a dual beam principle where ceramic material is removed in a molten form. However, the laser beams produces large temperature gradients in the workpiece that results in surface and sub-surface damage. Another alternative has been abrasive jet machining. This process uses high pressure abrasives to pierce and wash away ceramic material[3]. Unfortunately, wide use on the shop floor is limited due to the influence of economic constraints and the availability of new equipment. The traditional, yet popular, machining process for ceramics is grinding. It is an abrasive machining operation where small chip fragments are produced by the cutting edges of tiny abrasive particles on the grinding wheels. The particles are hard structural ceramic materials such as Si_3N_4, SiC, and

alumina (a hot pressed silicon nitride ceramic) with consistently high levels of performance and dimensional accuracy. This enables grinding to achieve high quality microfinishing[4]. However, the usual drawback is low production rate. The brittle nature of ceramics also causes the grinding process to be susceptible to the formation of surface microcracks during machining. The cracks often lead to premature failure of the ceramic components during service. Current understanding of machining mechanisms on ceramic material is still limited. Research is necessary in the development of machining technologies for the processing of advanced ceramic materials to achieve cost reduction and quality assurance [5-8].

This paper presents an investigation of fundamentals behind the machining of advanced ceramic materials. The experimental work is based on a single-point turning process of aluminum oxide (Al_2O_3) bars. Polycrystalline, diamond-tipped, carbide inserts comprise the cutting edges on the cutting tool. Cutting forces are measured during the machining process and collected chip fragments are analyzed. A fracture-dominant mechanism to describe the material removal process is suggested. Fundamentals of chemical-assisted machining, for controlling the process of microcrack initiation and propagation, are investigated as a case study to demonstrate the application of this research.

BASIC METHODOLOGY OF INVESTIGATION

The main objective of this investigation is to gain a comprehensive understanding of the fundamental principles in machining ceramics. Starting from the selection of aluminum oxide (Al_2O_3) as the testing material, our research continues to search for proper tool insert materials, establish the machining setup, and determine machining conditions for the material removal process.

Selection of Ceramic Materials

Ceramic materials are characterized as difficult-to-machine materials because of their high hardness and brittleness. Aluminum oxide (Al_2O_3) is selected as the test material because it is commercially used in applications of corrosive environments with elevated temperatures. The test specimens are prepared as cylindrical bars having diameter = 19.0 mm and length = 76.2 mm. The material contains 99.8% pure α - alumina with impurities that primarily consist of magnesium oxide as a sintering aid. The grain size is 10-12 μm.

Selection of Tool Materials

It has been well known that the material properties of the cutting tool dictate the qualification of tools which can be used in a given machining process. The most noted property is the insert material hardness, especially the hardness under high temperature conditions. In our study of turning aluminum oxide (Al_2O_3), two types of tool inserts are used: polycrystalline, diamond-tipped, carbide inserts and cubic boron nitride (CBN) inserts. The former sustained the machining action during the tests, but the CBN tool inserts did not. Table 1 provides a comparison of hardness, modulus of elasticity, flexural strength, and fracture toughness between the two materials. Note that the major difference is in material hardness. The hardness of diamond material is much higher than the hardness of CBN material, although, the CBN inserts possess a higher value of flexural strength than do the diamond inserts. By comparing the difference in hardness between the aluminum oxide and the diamond material listed in Table 1, a conclusion can be drawn that a minimum ratio of the tool hardness to the hardness of the ceramic material being machined should be maintained at a minimum of 5:1 or 6:1. Diamond is, therefore, recommended because it is the hardest known material. Diamond also possesses the largest thermal conductivity and chemical inertness, two important requirements of machining tool materials.

TABLE 1: TOOL INSERT MATERIALS AND ALUMINUM OXIDE COMPARISON

Mechanical Property Item	Unit	Aluminum Oxide	Polycrystalline Diamond Compact	Cubic Boron Nitride (CBN)
Hardness	GPa	11-12	60-90	29
Modulus of Elasticity	GPa	345	725-1049	680
Flexural Strength	MPa	359	500	750
Fracture Toughness	$MPa*\sqrt{m}$	4.0	3.4	-
Grain Size	μm	10-12	-	-

Experimental Procedures

To study the material removal mechanisms, the investigation focuses on the following issues:

1. Cutting force generated during machining.
2. Formation of surface texture formed during machining.
3. Exploration of a new machining technology that ensures surface quality and provides adequate machining efficiency.

Figure 1 illustrates that the aluminum oxide (Al_2O_3) bars are machined on a CNC Slant lathe. An instrumented tool post with attached strain gage sensors is used to perform in-process cutting force measurements. A special cutting fluid system is used for feeding cutting fluid into the cutting area and collecting chip fragments through a filtering device. A PC-based computer data acquisition system records the cutting force signal. A factorial design method [9] is used with three fundamental cutting parameters as the independent variables. The parameters are feed, depth of cut, and cutting speed. Table 2 lists the eight combinations of the three machining parameter settings and the measured cutting force data in both the cutting speed and feed directions.

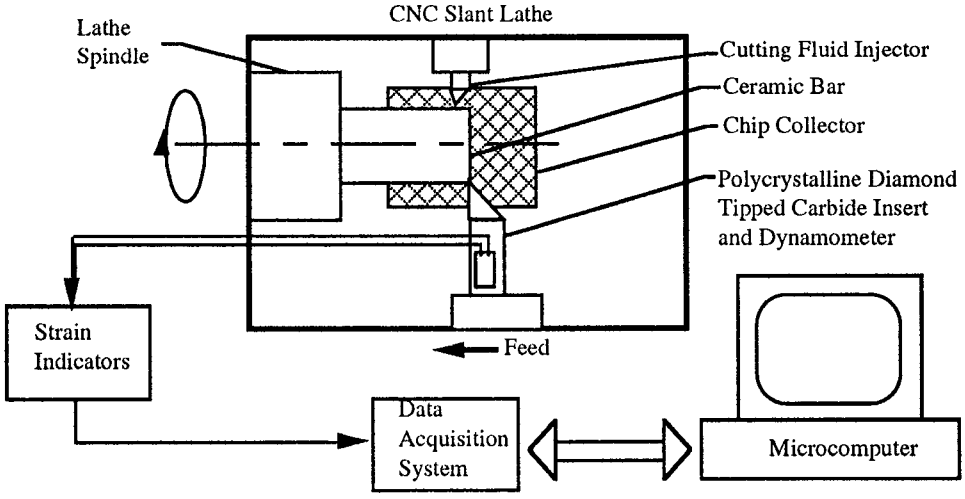

FIGURE 1: EXPERIMENTAL SETUP FOR MACHINING ALUMINA

TABLE 2: DATA OF CUTTING FORCE MEASUREMENTS WITH DISTILLED WATER AS CUTTING FLUID

Test No.	Cutting Parameters			Tangential Force, Ft, N	Feed Force, Ff, N	Resultant Force, N	Unit Cutting Force, MPa	Ratio of Ft/Ff
	d,mm	f,mm/min	v, rpm					
1	0.1	5.	400.	61.	69.	92.1	184.2	0.88
2	0.2	5.	400.	71.	122.	141.2	141.2	0.58
3	0.1	10.	400.	76.	73.	105.4	105.4	1.04
4	0.2	10.	400.	79.	123.	146.2	73.1	0.64
5	0.1	5.	600.	53.	72.	89.4	178.8	0.74
6	0.2	5.	600.	80.	116.	140.9	140.9	0.69
7	0.1	10.	600.	65.	70.	95.5	95.5	0.93
8	0.2	10.	600.	102.	114.	153.0	76.5	0.89

ANALYSIS OF MACHINING MECHANISMS

In this section, results obtained from the cutting force measurements are analyzed. Emphasis is given to the discussion of "What are the mechanics that best describe the material removal process?".

Important Observations

The machining mechanism observed during the machining of metals indicates that whenever a cutting tool cuts into the workpiece material, elastic deformation begins and three deformation zones are formed as stresses build up in the material. The unit cutting force, as a normalized index for characterization, is defined as a ratio of the cutting force to the cutting area. In machining conventional materials such as metal, the unit cutting force needed to carry out the material removal process can be estimated from the ultimate tensile strength of the material being machined. In most cases, the ratio of the unit cutting force to the ultimate tensile strength ranges from 1.5 to 4.0 when the chip compression factor remains below 2.0 [10].

In the machining of aluminum oxide (Al_2O_3), the presence of chips, the formation of surface texture, and the tool wear observed on rake and frank faces support the existence of the three deformation zones. Nevertheless, by examining the measured unit cutting force, the numerical data are far below the ultimate tensile strength of the aluminum oxide material being machined. This is a characteristic of fracture failure. Table 2 indicates that the average of the measured unit cutting forces at the 8 testing conditions is about 124.5MPa. This is only about 35% of the 359 MPa of the flexural strength of aluminum oxide listed in Table 1. More interesting to note is that increasing the depth of cut results in a decrease in the observed unit cutting force. In addition, there is no significant effect of cutting speed on the unit cutting force. These phenomena are contradictory to what have been noticed in machining conventional materials. Therefore, the material removal process during the machining of ceramics can not be simply explained with metal cutting principles. There must exist some mechanism(s) during the machining of ceramic materials that are different from those observed during the machining of conventional materials (e.g. machining metals).

Interpretation of Machining Mechanisms

This research applies the theory of fracture mechanics to gain a basic understanding of the mechanics of the material removal process during the machining of ceramics. The testing material used in this study is alumina oxide. The material, being a brittle solid, has its inherent fracture toughness. It has been known that the inherent fracture toughness can decrease significantly with increasing loading rate. Figure 2 presents a comparison of three fracture toughness curves obtained under three different loading rates, indicating the tendency of decreasing fracture

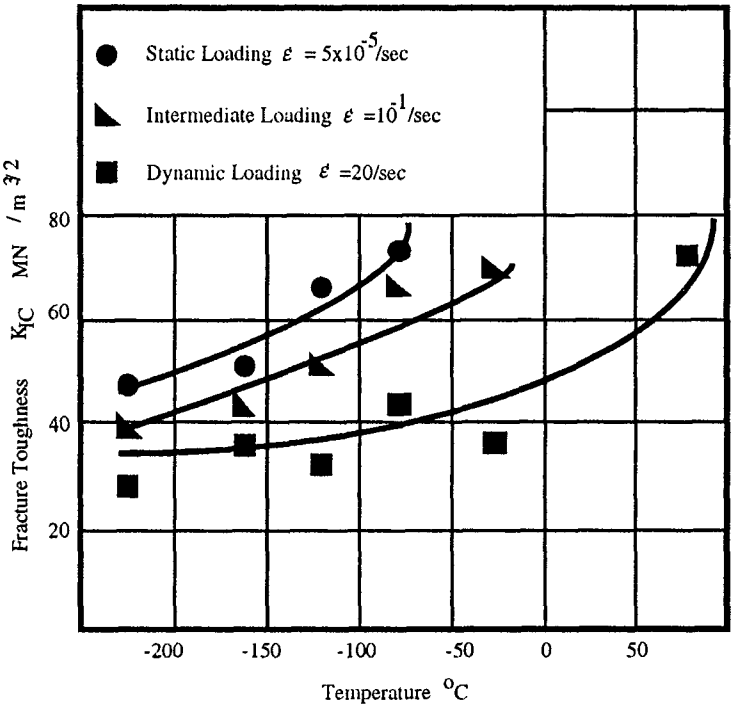

FIGURE 2: EFFECT OF THE LOADING RATE ON THE INHERENT FRACTURE TOUGHNESS OF AN ABS-C STEEL [11]

toughness as the loading rate increases[11]. Since a turning process is equivalent to applying a load to the workpiece by the cutting tool, a high cutting speed resembles a high loading rate. Consequently, the inherent fracture toughness of the ceramic workpiece decreases significantly. Fracture (not shearing) becomes a prevailing mechanism in the material removal process. To confirm this claim, chip fragments are collected during machining and examined using an environmental scanning electronic microscope (ESEM). Figures 3a and 3b show two representative types of chip. Examination of the lateral surfaces shows that they are typical brittle-fracture surfaces. This feature indicates that the chip formation during machining is a macro-scale fracture process, or that the chip is formed in a cleavage fracture mode. There exists a unique difference between these two types of chip. The chip shown in Fig. 3a has a smooth flat surface. The parallel lines (i.e. the plowing marks) on the smooth surface resemble the chip flow over the rake face of a cutting tool. This is a phenomenon routinely observed during machining of metals. This observation clearly shows that there is direct contact between this type of chip and the cutting tool during the chip formation process. It also implies that a significant amount of chip formed during machining does not contact the cutting tool directly. Under those circumstances, chip formation is only due to a fracture process characterized by crack initiation and propagation.

Model of Machining Mechanisms

From the above discussion, a model is proposed for describing the mechanics of material removal during the machining of ceramic material. An emphasis is placed on the relationships between the macroscopic and microscopic fracture behaviors. Figure 4 illustrates the five essential stages in this basic physical process.

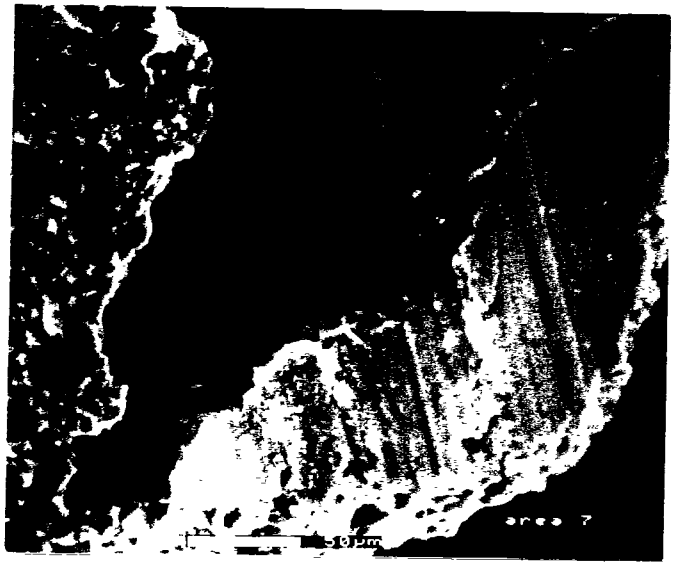

(a) MACHINED CHIP FORMED BY THE DIRECT CONTACT BETWEEN THE MATERIAL BEING REMOVED AND THE CUTTING TOOL

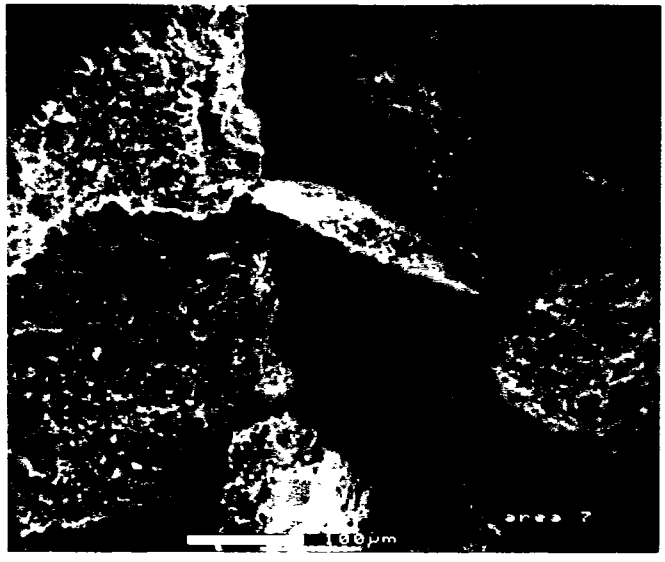

(b) FRACTURED CHIP FORMED WITHOUT DIRECT CONTACT BETWEEN THE MATERIAL BEING REMOVED AND THE CUTTING TOOL

FIGURE 3: TWO TYPES OF CHIP IDENTIFIED DURING THE MACHINING OF ALUMINA

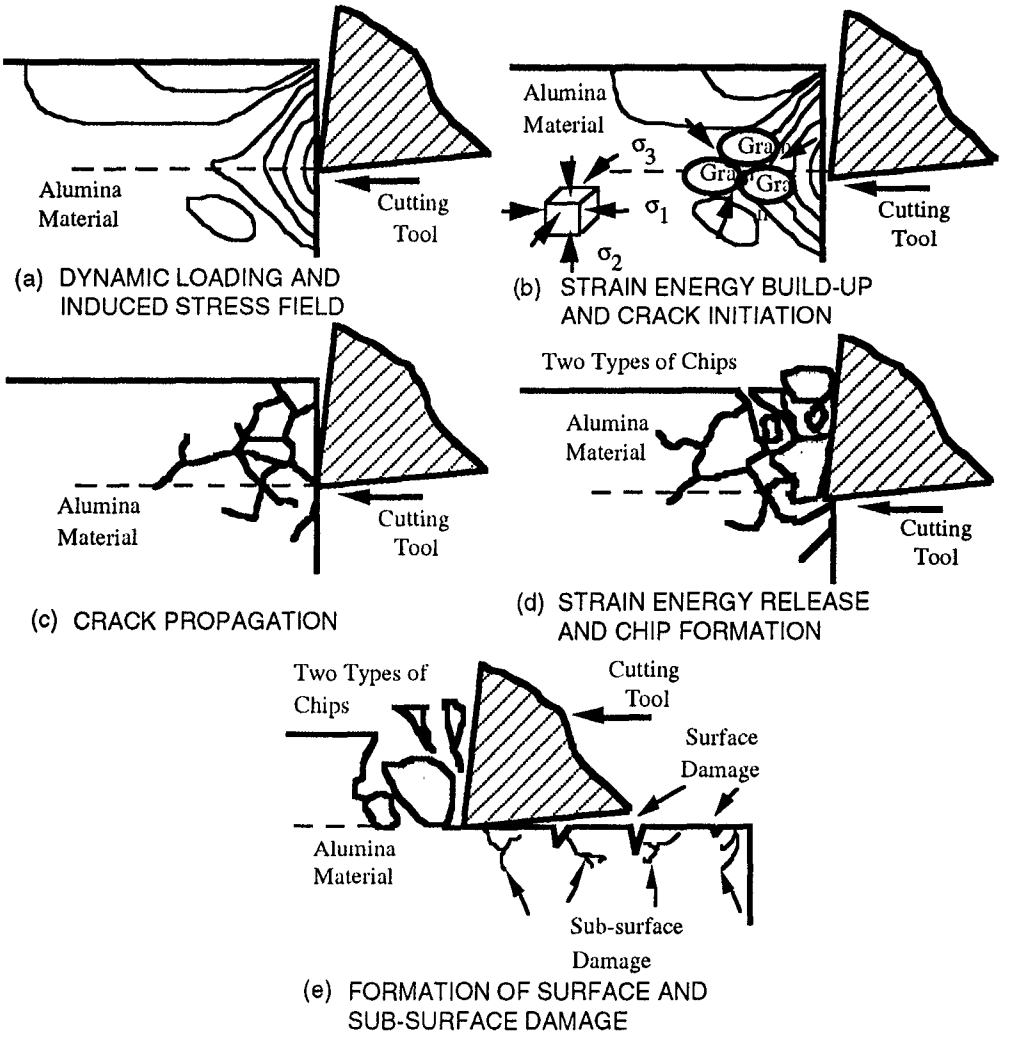

FIGURE 4: FIVE ESSENTIAL STAGES IN THE MATERIAL REMOVAL PROCESS

1. Dynamic Loading: The tool approaches the workpiece. The machining process begins when the tool touches the workpiece. The impact between them induces stresses in the workpiece material. The stresses form a stress field inside the workpiece (Figure 4a).
2. Strain Energy Built-up and Crack Initiation. The strain energy stored in the workpiece material accumulates as the cutting tool continues its movement. The strain energy is highest at locations where the hydrostatic pressure is very high. Once the induced stresses reach a critical level, the stresses initiate crack nucleation. The crack sites are locations of stress singularities where high internal tensile stresses accumulate. These locations can take the form of triple-point junctions, dislocation pile-ups at grain boundaries, or second-phase particles. All of these locations are sites of the stress concentration and pose the initiation of microcracks (Figure 4b).

3. Crack Propagation: As the machining process progresses and stresses continue to develop in the material, microcracks propagate through the immediate surrounding material. Both intergranular and transgranular cracks develop. Cracks continue to propagate until obstacles are encountered such as grain boundaries(Figure 4c).
4. Strain Energy Release and Chip Formation: The process of crack propagation is completed when more microcracks merge and form chip fragments. The collapse of the dynamic equilibrium of strain at the hydrostatic point during the crack propagation creates unique opportunities to release the stored strain energy. Its sudden release usually leads to a catastrophic failure mode, resembling a micro-scale explosion, thus promoting crack propagation. The size of particles formed in the catastrophic failure mode depends on the strain energy stored per unit volume in the stress field. The higher the strain energy stored, the finer the particle formed. Consequently, in the chip formation process, the material separated by fracture can be either next to the rake face of the cutting tool or away from it depending on the pattern of stress distribution. Two types of chip are formed as a result. The type of machined chip (shaded chip fragments) represents the fractured material directly beneath the tool action, and is also subjected to the influences of temperature. On the other hand, fractured chip type is governed by the stress distribution and the material microstructure (Figure 4d).
5. Formation of Surface and Sub-surface Damage: Chip fragments are formed during machining due to brittle fracture. This causes concurrent formation of cracks in the surface texture of the machined surface. These cracks are called surface damage and, in general, unavoidable during machining of ceramic materials. In addition, the residual effects of brittle fracture near the surface layer bury numerous microcracks to a certain depth leading to sub-surface damage (Figure 4e).

INVESTIGATION OF SURFACE TEXTURE FORMATION

One of the ultimate objectives of machining ceramics is to achieve a high degree of geometrical accuracy with a designed part. The texture formed on a machined surface plays a key role in this regard. Based on the previous discussion, the machined surface is an assemblage of fracture surfaces left behind by chip formation.

Volumetric Distribution of Chip

A systematic examination of the number of chip fragments formed during machining is now discussed. Chip fragments collected during machining are uniformly laid on a flat sample holder under an ESEM. The number of chip fragments for a given area is counted and the size of each fragment is measured. A threshold is selected to distinguish large, medium, and small chip fragments. Figure 5a displays two distributions of chip size at a normalized scale of 100 fragments. These two distributions are associated with two machining conditions which have a different setting for depth of cut. As illustrated in Figure 5a, the percentage of small fragments decreases from 80% to 60% as the setting of depth of cut increases from 0.1 mm to 0.2 mm. On the other hand, the percentage of large fragments increases from 8% to 16% as the setting of depth of cut increases. Figure 5b presents the percentage of volume contributed by the small, medium, and large fragments. It is evident that the material removed by setting of depth of cut to 0.2 mm during machining mainly produces large chip fragments (42.8% as shown in Figure 5b). Note that the large chip fragments usually belong to the type of machined chip that indicates a tendency of leaving microcracks on the machined surface. One important finding of this study is the strong correlation between the surface finish and the size variation of chip fragments. There is, although, no strong correlation between the surface finish and the mean value of chip size. It is illustrated in Figure 5c that a low variation of chip size is constantly associated with a low value of Ra measurement. This finding implies that the control of finish quality on machined surfaces can be achieved through minimizing the chip size variation.

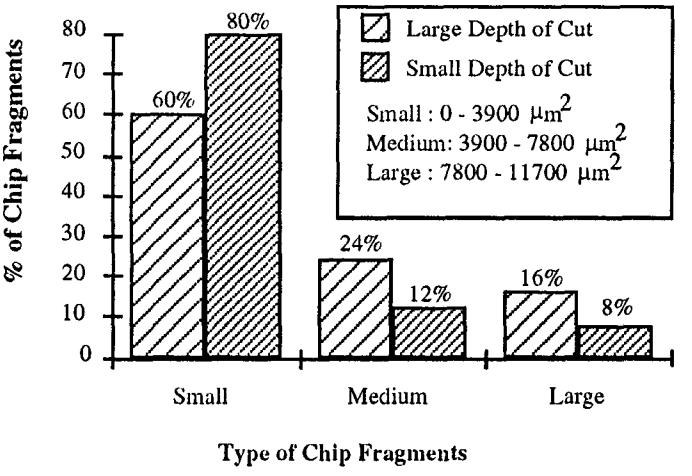

(a) DISTRIBUTION OF CHIP FRAGMENTS

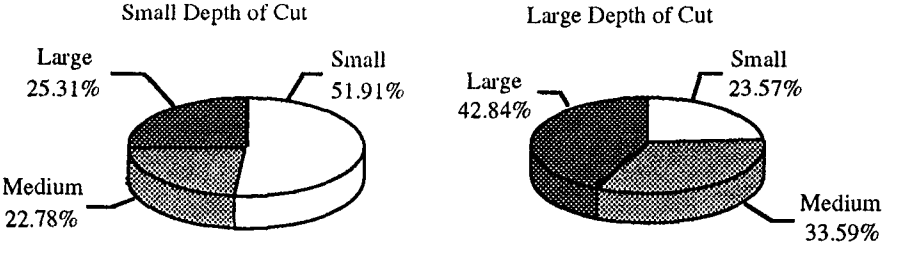

(b) VOLUMETRIC DISTRIBUTION OF CHIP FRAGMENTS

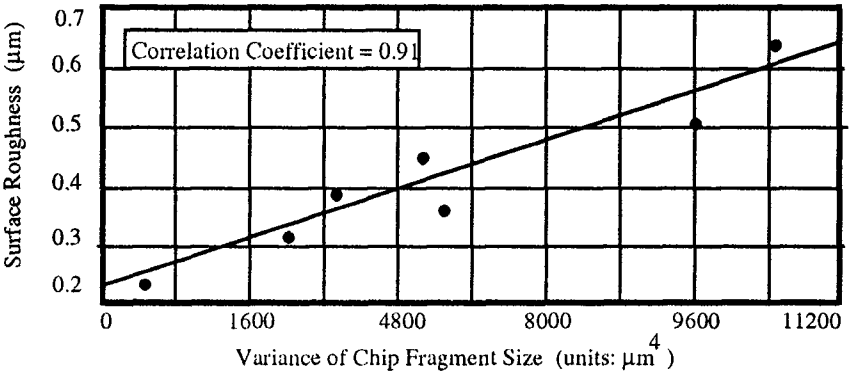

(c) CORRELATION BETWEEN THE CHIP SIZE VARIATION AND R_a VALUE

FIGURE 5: DISTRIBUTION OF CHIP SIZE AND VOLUME WITH RELATION TO ROUGHNESS AVERAGE

Stereophotogrammetric Examination of the Surface Texture through Image Processing

The machined surfaces obtained under the eight machining conditions are examined by ESEM techniques. The eight micrographs shown in Figure 6 are the images taken from the surfaces (magnification at x500). To visualize the formed surface texture, we utilize a method called stereophotogrammetric examination, which offers a direct and nondestructive procedure for determining the elevation of a fracture surface at selected regions [12-14]. This research incorporates the development of a software package that integrates image processing, profilometry, and computer graphics to quantify the size and shape of intergranular and transgranular cracks from the ESEM micrographs. The package generates an isometric view to produce the three-dimensional features of the surface texture. This is usually lost or buried in regular two-dimensional surface measurements. Contour maps of the surface are also generated in order to provide three-dimensional information from a different perspective. Figures 7a and 7b present a visualized surface texture and an associated contour map. The corresponding area of the surface texture is marked in the micrograph shown in Figure 6e. The reconstructed fracture surface texture vividly depicts the appearance of surface cracks and quantifies the relative positions between the surface roughness and the surface cracks. The contour lines in the contour map shown in Figure 7b contain 0.5 μm intervals. The numbers displayed outside the frame are the location heights. The lowest point of the surface topography is 0.0 μm. The pixel number (Figures 7a and 7b), provides a scale for calculating dimensions in a horizontal plane. Adding the width between two contour lines provides a quantitative information about the size and shape of a crack. For example, the width marked as 0.4μm in Figure 8b covers 6 contour lines. The information provides the size of a V-shaped crack having an angle of 7.6° with its vertex located 4.2 μm away from the reference plane for R_a measurements. It is interesting to note that the contour map can assist us in identifying transgranular cracks. For example, the boundaries of a 10 μm grain can be identified on the map shown in Figure 7b. A 0.8 μm crack path is also identified within the grain. The stereophotogrammetric examination through image processing provides a powerful tool to establish the quantitative relationships between the crack formation and machining conditions.

GUIDELINES OF MACHINING CERAMIC MATERIAL

Based on the comprehensive understanding of the fracture-based material removal mechanisms, several guidelines for machining ceramic material are suggested as follows:

1. The cutting tool material must possess a hardness value as high as three times the hardness value of the ceramic material being machined. Otherwise, accelerated wear not only increases tooling cost, but also deteriorates the machining performance significantly by inducing surface and sub-surface damage.
2. Machining parameters, such as depth of cut, feed, and cutting speed have significant effects on machining performance. In general, large depth of cut causes a high percentage of large chip fragments. High cutting speed increases the loading rate, thereby, accelerating the build-up of hydro-static pressure, and increasing the occurrence of catastrophic failure during crack propagation. This leads to high production of small chip fragments, indicating the presence of short-crack regions [15]. As the short cracks extend, the fracture toughness of alumina increases and resists extension of the developed cracks. Consequently, on a macro-scale, the cutting speed does not show significant effects on the unit cutting force required to remove the material. To take advantage of short-crack initiation, machining ceramics at high cutting speed will be recommended only under conditions where a small depth of cut is used.
3. Finish quality of machined surfaces can be improved by controlling the variation of chip size. Ductile region grinding is a typical example of maintaining the formation of small chip fragments. Tensile stresses are necessary for brittle fracture to occur. Therefore, measures taken during machining that affect the stress distribution in the cutting zone will have the potential to control the machining performance. Reduction of the residual tensile stress on and beneath the machined surface prolongs the life cycle of the machined part.

(a) d = 0.772 mm
v = 67.0 m/min

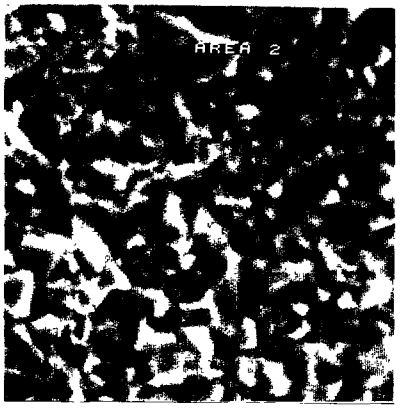

(b) d = 0.772 mm
v = 11. m/min

(c) d = 0.264 mm
v = 67. m/min

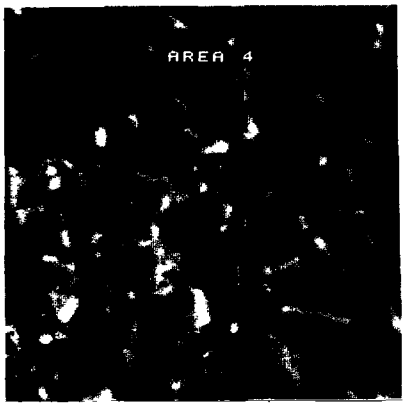

(d) d = 0.264 mm
v = 11. m/min

FEED = 0.012 mm/rev

FIGURE 6: MICROGRAPHS FOR THE SURFACE FINISH FROM EIGHT DIFFERENT MACHINING CONDITIONS

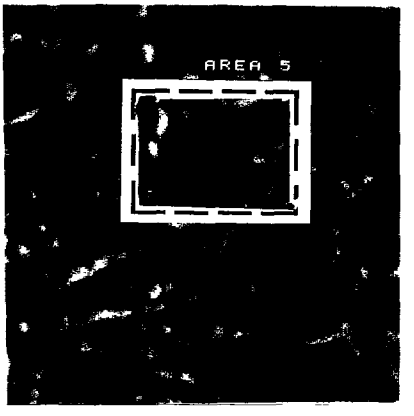

(e) d = 0.772 mm
v = 67.0 m/min

(f) d = 0.772 mm
v = 11. m/min

(g) d = 0.264 mm
v = 67. m/min

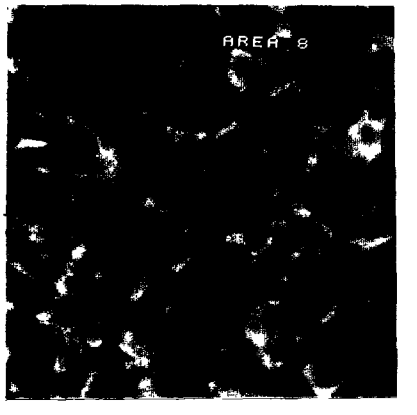

(h) d = 0.264 mm
v = 11. m/min

FEED = 0.051 mm/rev

FIGURE 6(contd): MICROGRAPHS FOR THE SURFACE FINISH FROM EIGHT DIFFERENT MACHINING CONDITIONS

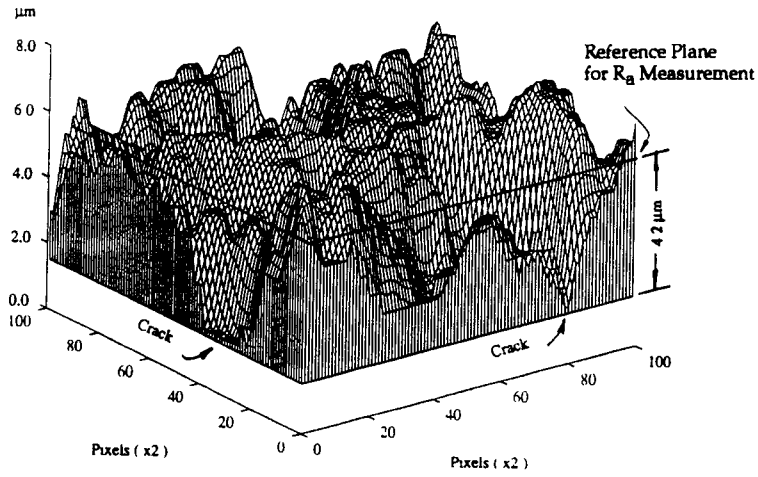

(a) VISUALIZATION OF SURFACE TOPOGRAPHY AND CRACK INDICATIONS

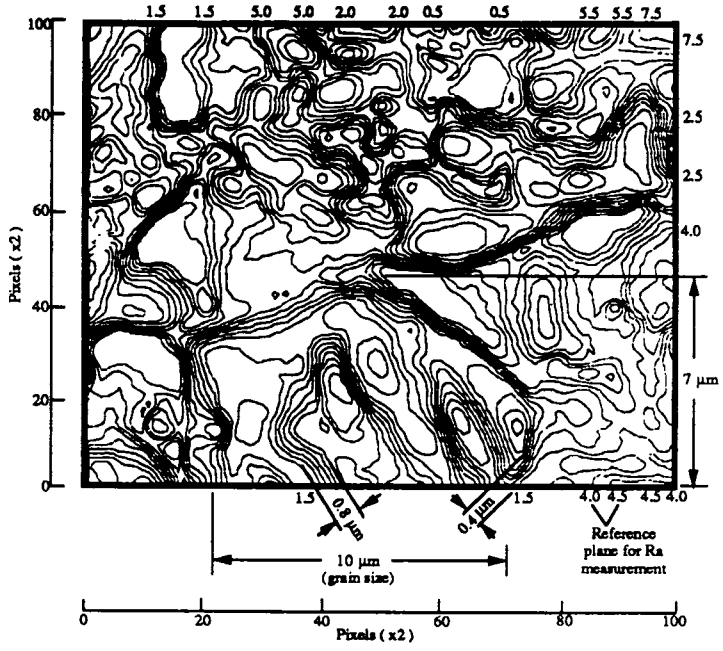

(b) CONTOUR MAP FOR QUANTIFYING THE FORMED CRACKS

FIGURE 7: VISUALIZED SURFACE TEXTURE AND CONTOUR PLOT

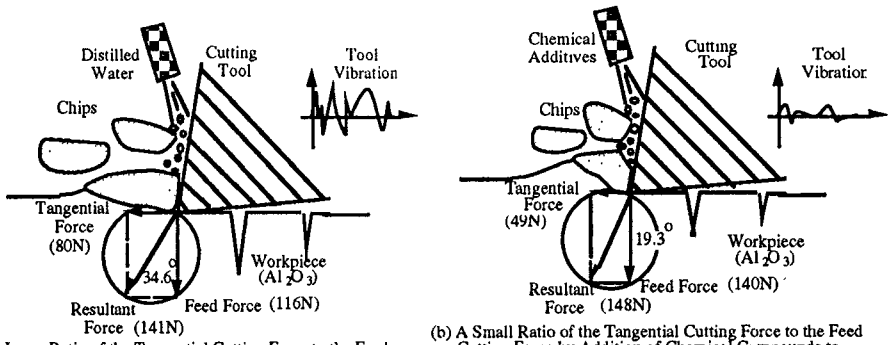

(a) A Large Ratio of the Tangential Cutting Force to the Feed Cutting Force when Using Distilled Water as Cutting Fluid

(b) A Small Ratio of the Tangential Cutting Force to the Feed Cutting Force by Addition of Chemical Compounds to Distilled Water

FIGURE 8: EFFECT OF BORIC ACID ADDITIVE ON FORCES DURING MACHINING

As a demonstration example, a case study of chemical-assisted machining is presented[16]. Boric acid is mixed with distilled water to serve as the cutting fluid during machining. The interaction between boric acid and the polycrystalline diamond compact of the cutting tool alters the tribological interaction on the interface between the cutting tool and the workpiece. As shown in Figure 8, the friction force increases with the presence of boric acid. High intensity tensile stresses that were developed in a thin layer near the surface controlled crack initiation and directed the crack propagation along the cutting speed direction. The chemical interaction between the boric acid and the amorphous oxide grain boundary phase in polycrystalline alumina promoted intergranular fracture. Experimental data shows that as material removal rates increased, the surface quality improved significantly [16].

CONCLUSIONS

Provided in this research is a fundamental study related to machining ceramic materials. Major conclusions are summarized as follows:

1. Machining of ceramic materials is characterized by a five-stage process; dynamic loading, strain energy build-up and crack initiation, crack propagation, chip formation, and surface texture generation. Fracture, instead of shearing, is the dominant mechanism in the material removal process.
2. There are two types of chip that form during machining; the machined chip and the fractured chip. The fractured chip is formed in a catastrophic failure mode that is triggered by sudden release of the strain energy stored in the ceramic material being machined.
3. In order to process ceramic material efficiently, machining must be adapted with specific characteristics of the ceramic material (i.e. hardness and brittleness). Demand for understanding material-specific removal mechanisms continues to influence the development of new and cost-effective machining technologies.

ACKNOWLEDGMENTS

The authors acknowledge the support of the University of Maryland Research Board, the Department of Mechanical Engineering, and the Institute for Systems Research at the University of Maryland under Engineering Research Centers Program: NSFD CDF 8803012. Special thanks are due Mr. Myron E. Taylor, Director of the Central Facility for Microanalysis, who provided valuable assistance in conducting the SEM study. The assistance from Mr. Michael Woodruff during the course of this work is also appreciated.

REFERENCES

1. Chryssolouris, G., Bredt, J., Kordas, S., and Wilson, E., "Theoretical Aspects of a Laser Machine Tool," *ASME Winter Annual Meeting Proceedings*, PED 20, December 1986, pp. 177-190.
2. Konig, W., and Zaboklicki, "Laser-assisted Hot Machining of Ceramics and Composite Materials," *Proceedings of the International Conference on Machining of Advanced Materials*, July 20-22, 1993, U.S., pp. 455-464.
3. Mazurkiewicz, M., "Understanding Abrasive Waterjet Performance," *Machining Technology*, Vol. 2, No.1, 1991, pp. 1-3.
4. Konig, W., and Popp, M., "Precision Machining of Advanced Ceramics," *Ceramic Bulletin*, Vol. 68, No. 3, pp. 550-553, 1989.
5. Hu, K., and Chandra, A., "A Fracture Mechanics Approach to Modeling Strength Degradation in Ceramic Grinding Processes," *Journal of Engineering for Industry*, Vol. 115, Feb., 1993, pp. 73-83.
6. Conway, J., and Kirchner, H., "Crack Branching as a Mechanism of Crushing During Grinding," *Journal of American Ceramics Society*, 69 [8], pp. 603-607.
7. Subramnian, K., and Ramanath, S., "Principles of Abrasive Machining Processes," Vol. 4, *Ceramics and Glasses*, American Society of Manufacturers Hand Book, 1991.
8. Evans, A., and Marshall, D., "Wear Mechanisms in Ceramics," *Fundamentals of Friction and Wear*, Ed. D. Rigney, American Society of Metals, 1980, pp. 439-452.
9. Box, G., et al., "*Statistics for Experimenters: An Introduction to Design, Data Analysis, and Model Building*," John Wiley & Sons, 1978.
10. Kronernburg, M., "*Machining Science and Applications*," Pergamon Press, 1966.
11. Barsom, J. and Rolfe, S., "*Fracture and Fatigue Control in Structures*," Second Edition, Prentice-Hall, 1987.
12. Underwood, E.E., "Recent Advances in Quantitative Fractography," Part 2, in "*Fracture Mechanics: microstructure and micromechanisms*," Edited by Nair, et al, ASM International, 1989, pp. 87-109.
13. Underwood, E.E., "Quantitative Fractography," Chapter 8, in "*Applied Metal-lography*," G.F. Vander Voort, Ed., Van Nostrand Reinhold, 1986, pp. 101-122.
14. Hilliard, J.E., Quantitative Analysis of Scanning Electron Micrographs," *Journal of Microscience*, 95, Part 1, 1972, pp. 45-58.
15. Lawn, B., "*Fracture of Brittle Solids*," Second Edition, Cambridge University Press, Cambridge, 1993.
16. Zhang, G.M., Hwang, T.W., and Anand, D.K., "Chemo-Mechanical Effects on the Efficiency of Machining Ceramics," *Proceedings of 1993 National Science Foundation Design and Manufacturing Systems Conference*, Charlotte, NC, Januaary, 1993, pp. 421-428.